Femtosecond single-shot imaging and control of a laser-induced first-order phase transition in HoFeO$_3$

Afanasiev, D.; Ivanov, B. A.; Pisarev, R. V.; Kirilyuk, A.; Rasing, Th; Kimel, A. V.

PAPER • OPEN ACCESS

Femtosecond single-shot imaging and control of a laser-induced first-order phase transition in HoFeO$_3$

To cite this article: D Afanasiev *et al* 2017 *J. Phys.: Condens. Matter* **29** 224003

View the article online for updates and enhancements.

IOP ebooks™

Bringing you innovative digital publishing with leading voices to create your essential collection of books in STEM research.

Start exploring the collection - download the first chapter of every title for free.

Femtosecond single-shot imaging and control of a laser-induced first-order phase transition in HoFeO$_3$

D Afanasiev[1,2]**, B A Ivanov**[3,4]**, R V Pisarev**[5]**, A Kirilyuk**[6]**, Th Rasing**[6] **and A V Kimel**[6]

[1] Radboud University, Institute for Molecules and Materials, 6525 AJ Nijmegen, Netherlands
[2] Kavli Institute of Nanoscience, Delft University of Technology, PO Box 5046, 2600 GA Delft, Netherlands
[3] Institute of Magnetism, National Academy of Sciences, 03142 Kiev, Ukraine
[4] Taras Shevchenko National University of Kiev, 01601 Kiev, Ukraine
[5] Ioffe Physical-Technical Institute, Russian Academy of Sciences, 194021 St. Petersburg, Russia
[6] Radboud University Nijmegen, Institute for Molecules and Materials, 6525 AJ Nijmegen, Netherlands

E-mail: d.afanasiev@tudelft.nl

CrossMark

Abstract

Excitation of antiferromagnetic HoFeO$_3$ with a single 80 fs laser pulse triggers a first-order spin-reorientation phase transition. In the ultrafast kinetics of the transition one can distinguish the processes of impulsive excitation of spin precession, nucleation of the new domain and growth of the nuclei. The orientation of the spins in the nuclei is defined by the phase of the laser-induced coherent spin precession. The growth of the nuclei is further promoted by heating induced by the laser excitation. Hereby we demonstrate that in HoFeO$_3$ coherent control of the spin precession allows an effective control of the route of the heat-induced first-order magnetic phase transition. The theoretical description of the excitation of the spin precession by linearly-polarized ultrashort laser pulses is developed with the sigma model. The analysis showed high sensitivity of the excited dynamics to the initial spin orientations with respect to the crystallographic axes of the material.

(Some figures may appear in colour only in the online journal)

1. Introduction

Ultrafast magnetism, starting from the seminal observation of subpicosecond demagnetization of Ni films [1], has developed into a rapidly growing scientific area in the last two decades with a potential to impact modern digital technology. Due to their rich phase diagram rare-earth orthoferrites have became one of the model systems in ultrafast magnetism [2–4]. The spatio-temporal visualization of the laser-induced spin dynamics with femtosecond temporal resolution was shown to be crucial for understanding the ultrafast kinetics of the phase transitions [5–8]. Reorientation of the weak magnetic moment in antiferromagnetic rare-earth orthoferrites via a second-order phase transition was studied with both spatial and femtosecond temporal resolution for (Sm,Pr)FeO$_3$ in [9]. Femtosecond imaging of the first-order phase transition from a collinear to a non-collinear antiferromagnetic state in DyFeO$_3$ was reported in [10]. HoFeO$_3$ is another compound from the family of rare-earth orthoferrites which has an unusual spin-reorientation phase transition. Although the spin reorientation is similar to the one reported in [10], a net magnetization is present in both phases and thus can be manipulated by means of an external magnetic field. It is thus of special interest to investigate the ultrafast kinetics of the

first-order spin-reorientation phase transition in HoFeO$_3$ and compare it with the results obtained earlier for (Sm, Pr)FeO$_3$ and DyFeO$_3$.

Here we investigate in detail ultrafast kinetics of the photo-induced first-order spin-reorientation phase transition in dielectric HoFeO$_3$. We show that a single linearly polarized laser pulse can launch the spin-reorientation and drive the collective spin rotation over 90 degrees. All-optical control of the magnetization in the photo-induced state can be achieved by varying the linear polarization of the pumping light and the sign of the magnetization in the ground state. We demonstrate that ultrafast time-resolved imaging of the photo-induced magnetization reveals stages of nucleation and consequent growth of the nuclei. These stages are typical for the kinetics of first-order phase transitions. The magnetization growth is accompanied by the coherent spin precession. The theoretical description of the excitation of the spin precession by linearly polarized laser pulses is developed with the sigma model, which takes into account the full magnetic symmetry of HoFeO$_3$. The analysis showed the high sensitivity of the excited dynamics to the initial spin orientations with respect to the crystallographic axes of the material. This is in good qualitative agreement with the main experimental results. We unambiguously demonstrate that while the magnetization growth is an incoherent process driven by the laser heating of the lattice, the sign of the magnetization in the growing nuclei is predefined by the phase of the coherent spin precession impulsively excited by the femtosecond laser pulse. This allowed us to conclude that the initial coherent oscillations are stimulus for the following orientation phase transition which consequently determine the spin orientation in the final magnetic phase. Unfortunately, the employed method of ultrafast imaging does not allow the spin dynamics at the sub-10 ps scale to be revealed. Presumably this is due to photo-induced birefringence which deteriorates the sensitivity of the measurements so that the images during the first 10 ps do not reveal any magnetic dynamics. As a result, the femtosecond imaging fails to detect the inertial dynamics reported in [11]. The sensitivity recovers afterward upon a relaxation of the photo-induced birefringence within 10 ps.

The paper is organized as follows. In section 2 we outline the main features of the spontaneous spin-reorientation transitions in HoFeO$_3$. In section 3 we describe our experimental set-up and show results of the static imaging of the domain structure of HoFeO$_3$ upon crossing the critical temperatures. In section 4 we demonstrate how the sign of the photo-induced magnetization can be controlled by the pump polarization and the direction of the magnetization in the ground state. Finally, in sections 5 and 6 we demonstrate the dynamics of the photo-induced magnetization and summarize the results.

2. Spontaneous spin-reorientation phase transitions in HoFeO$_3$

Holmium orthoferrite (HoFeO$_3$) crystallizes in an orthorhombic structure (point group is D_{2h}^{16}) [12]. Fe^{3+} spins are coupled antiferromagnetically. Due to the Dzyaloshinskii–Moriya

interaction the magnetizations $\mathbf{M}_1$ and $\mathbf{M}_2$ of the two magnetic sublattices acquire a relative canting over an angle of about 0.5 degrees. Due to the canting the antiferromagnet acquires a non-zero net magnetic moment $\mathbf{M} = \mathbf{M}_2 + \mathbf{M}_1$. The value and the direction of $\mathbf{M}$ is given by the relative orientation of the antiferromagnetic vector $\mathbf{L} = \mathbf{M}_2 - \mathbf{M}_1$ with respect to the crystallographic y-axis according to the relation:

$$\mathbf{M} = \frac{H_D}{H_{ex}} \mathbf{e}_y \times \mathbf{L}, \tag{1}$$

where H_D and H_{ex} are the Dzyaloshinskii and the exchange fields, respectively; $\mathbf{e}_y$ is a unit vector along the even axis of the crystal (the y-axis) [13, 14]. It is known that in a narrow temperature range from $T_1 = 39$ K to $T_3 = 58$ K the orthoferrite exhibits a number of magnetic phase transitions due to which the spins reorient from the z-axis to the x-axis [15–18]. Below $T_1 = 39$ K the spins are in the Γ_2 phase. In this phase $\mathbf{L}$ is oriented along the z-axis and $\mathbf{M}$ is oriented along the x-axis. In the temperature range from T_1 to $T_2 = 51$ K the antiferromagnetic vector gradually rotates in the $(1\,0\,0)$ plane ultimately acquiring an angle θ with the z-axis nearly equal to 30°. This angular phase is denoted as the Γ_{12} phase. At the temperature T_2 a first-order phase transition occurs during which the spins suddenly rotate toward the $(0\,1\,0)$ plane retaining the angle θ with the z-axis. This rotation results in an emergence of non-zero magnetization along the z-axis. The corresponding angular phase is denoted as Γ_{24}. A further increase of the temperature pulls the antiferromagnetic vector in the $(0\,1\,0)$ plane towards the x-axis. This rotation is accomplished at $T_3 = 58$ K when the spins are oriented along the x-axis and the net magnetic moment is pointing solely along the z-direction. This Γ_4 phase persists up to the Neel temperature $T_N = 647$ K [17]. Figure 1(a) schematically shows the whole set of the transitions between the magnetic phases in the range of temperatures from T_1 to T_3.

3. Experimental set-up and magneto-optical characterization of the sample

For the magneto-optical study of the spin-orientation phase transitions in HoFeO$_3$ we took a crystal cut perpendicularly to the z-crystallographic axis. The unfocused beam from an optical parametric amplifier at a central wavelength of 630 nm was used to probe the sample. The OPA was pumped by 80 fs laser pulses at the central wavelength of 800 nm from an amplified Ti:sapphire laser (Spectra Physics Spitfire). The repetition rate of the pulses was 1 kHz. A charge-coupled device (CCD) camera in combination with collective optics and two polarizers in the cross-Nicol configuration was used to visualize the magnetic structure by sensing the magneto-optical Faraday effect. The probing laser beam was nearly at normal incidence. Thus it is sensitive only to the out-of-plane magnetization component (z-component). It must be noted that in contrast to the measurements reported in [11], the sensitivity of this setup greatly depends on the orientation of the polarization of light with respect to the axis of the polarizer in front of the CCD camera. Below the temperature T_2 the
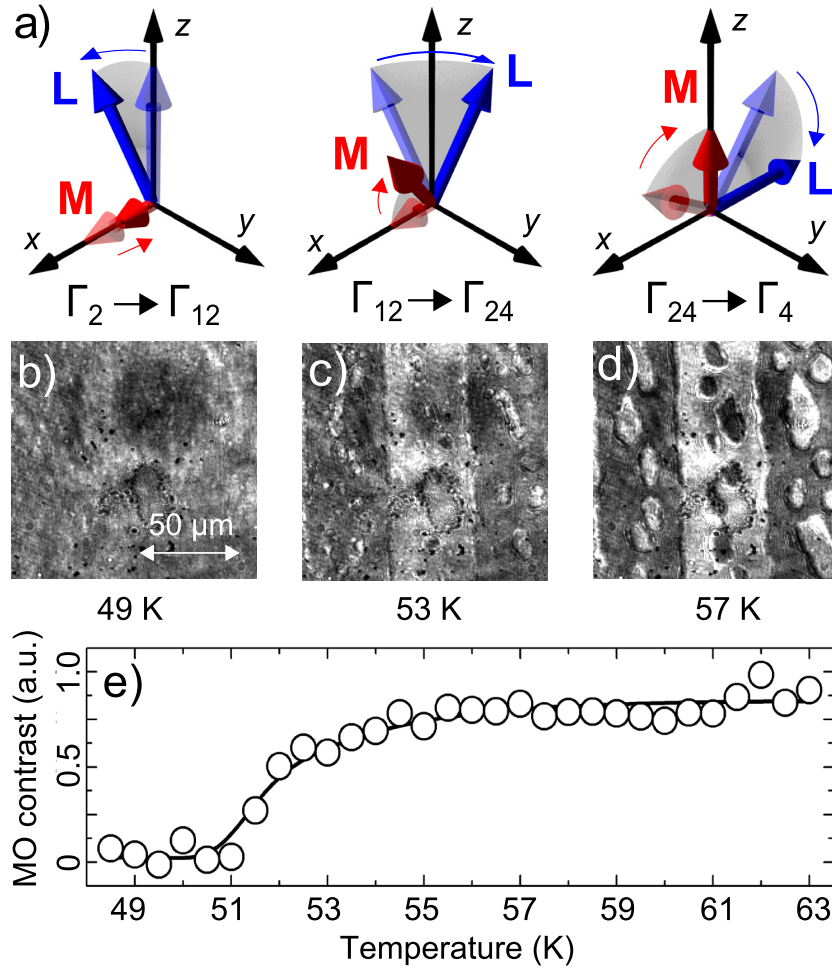
Figure 1. (a) Spin-reorientation magnetic phase transition in HoFeO$_3$. Each figure represents the transition from the initial (translucent) to the final (opaque) magnetic configuration. (b)–(d) Magneto-optical images of HoFeO$_3$ recorded at different sample temperatures. (e) The value of the magneto-optical contrast as a function of the sample temperature. The value is taken inside the area corresponding to the white magnetic domain at the elevated temperatures.

magnetic structure is characterized by the net magnetization oriented entirely along the *x*-axis. It cannot contribute to the Faraday effect and shows up as a homogeneous gray image (figure 1(b)). The emergence of the magnetization component along the *z*-axis results in a directly measurable Faraday rotation of the probe. This reveals an onset of the magnetic domain structure corresponding to the Γ_{24} phase (figure 1(c)). A gradual increase of the temperature results in an enhancement of the magneto-optical contrast while maintaining the main features of the domain structure (figure 1(d)). Naturally, the bright and dark areas on the images were assigned to the magnetic domains in which M_z points along and against the *z*-axis, respectively. Figure 1(e) summarizes the changes of the magneto-optical contrast as a function of temperature. It is seen that the contrast saturates at temperature nearly equal to 57 K. This value roughly agrees with the critical temperature T_3 [15].

In order to study the kinetics of the phase transition at an ultrafast timescale, we performed an all-optical pump–probe experiment. The sample was excited by a linearly polarized pump pulse with duration $\tau = 80$ fs. The central wavelength of the pump was 800 nm. The pump pulse had an incidence

angle close to 20 degrees. The beam had a Gaussian spatial profile, being focused into a spot with the full width at half maximum $\sigma = 75$ μm. The thickness of the sample d was equal to 70 μm. Similarly to [10], the repetition rate of the pump pulses was brought down to 2 Hz. The majority of the experiments was performed without external magnetic field.

4. Dependence of the photo-induced magnetic state on the polarization of the pump light and the antiferromagnetic vector

Figure 2(a) shows snapshots of the magneto-optical contrast in the low-temperature Γ_{12} phase at 48 K recorded 550 ps after the pump excitation. This time delay is long enough to guarantee that the magnetization is in thermal equilibrium with the lattice [19]. It is seen from the images that a single linearly polarized pump pulse produces well pronounced changes of the magneto-optical contrast. The laser fluence used in the experiment was 100 mJ cm^{-2}. The corresponding absorption results in local heating of the lattice of about 10 K. Such a temperature increase is sufficient to trigger the spin-reorientation phase transition. Accordingly, the pump-induced changes of the
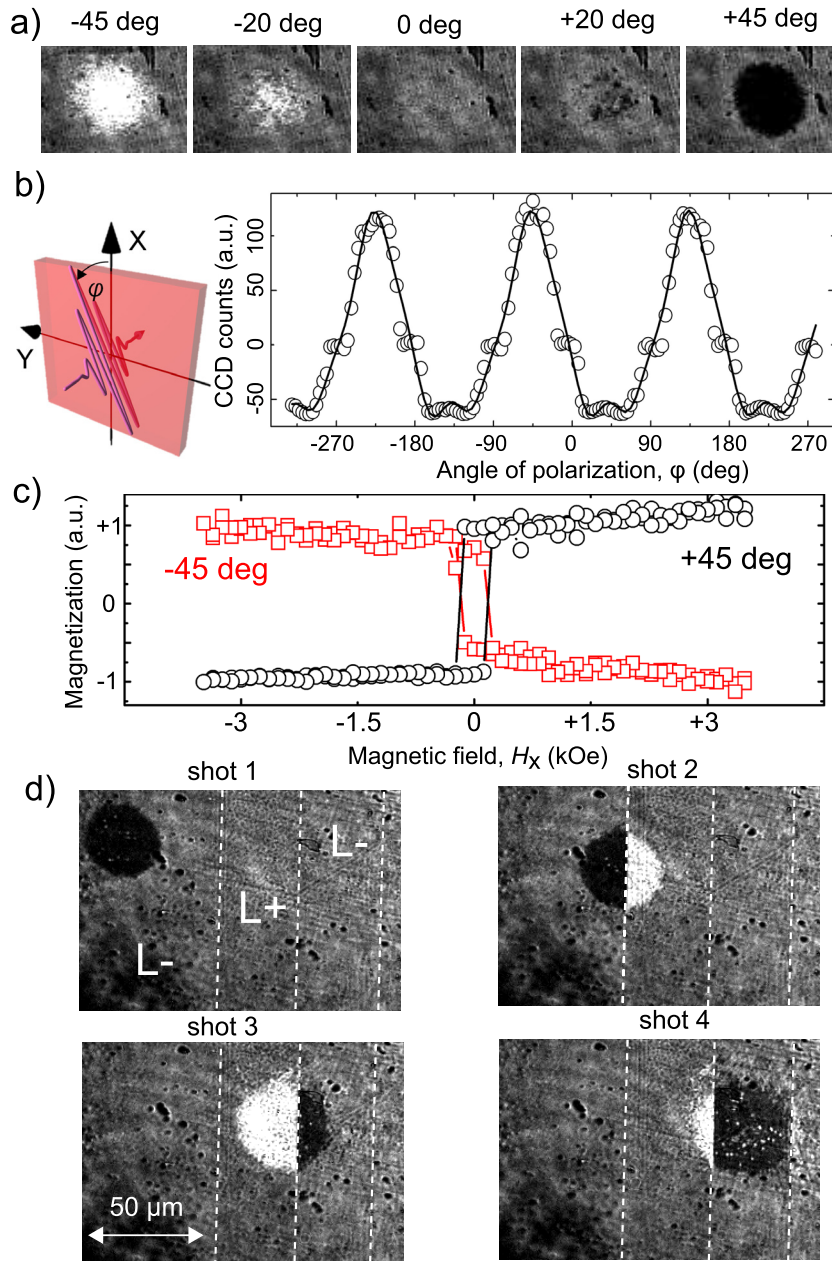
Figure 2. (a) Magneto-optical images of the photo-induced magnetic domains for various azimuthal orientations of the pump polarization. (b) The averaged change in the magneto-optical contrast over the spot as a function of the angle φ between the pump polarization and the *x*-axis. (c) The total magnetization averaged over the spot for various magnetic fields. The data are presented for the pump polarization having angle ± 45 degrees with the *x*-axis. (d) Images of the photo-induced domains taken at different sites of the sample. The pump polarization is oriented at 45 degrees with respect to the *x*-axis. The dashed lines represent boundaries of (here invisible) magnetic domains. The structure is revealed by the pump excitation. The images are taken 550 ps after the excitation with a 80 fs pump pulse. The sample temperature is 48 K.

Faraday rotation were attributed to the emergence of magnetization oriented along the *z*-axis (M_z). This magnetization is naturally inherited by the high-temperature phases (Γ_4 and Γ_{24}) and is not present in the low-temperature phases (Γ_2 and Γ_{12}). Because of the continuous nature of the transition $\Gamma_{24} \rightarrow \Gamma_4$ it is hard to unambiguously establish to which of these two phases the photo-induced magnetization belongs.

The photo-induced magnetization, shown in figure 2(a), demonstrates a strong dependence on the azimuthal angle φ which the polarization plane of the pump light makes with the *x*-axis (see figure 2(b)). To characterize changes in the photo-induced state quantitatively, images were digitized and averages were taken over the areas where the magneto-optical contrast had been changed. The polarization dependence has 180° periodicity with maxima for the azimuthal angles equal to ± 45 degrees. In order to study how the magnetic ground state affects the photo-induced magnetization, we applied a magnetic field H_x oriented along the *x*-axis. The field changes the sign of the net magnetization M_x and consequently the sign of the L_z projection of the antiferromagnetic vector in accordance with equation (1). Figure 2(c) demonstrates that the transient photo-induced magnetization is sensitive to the
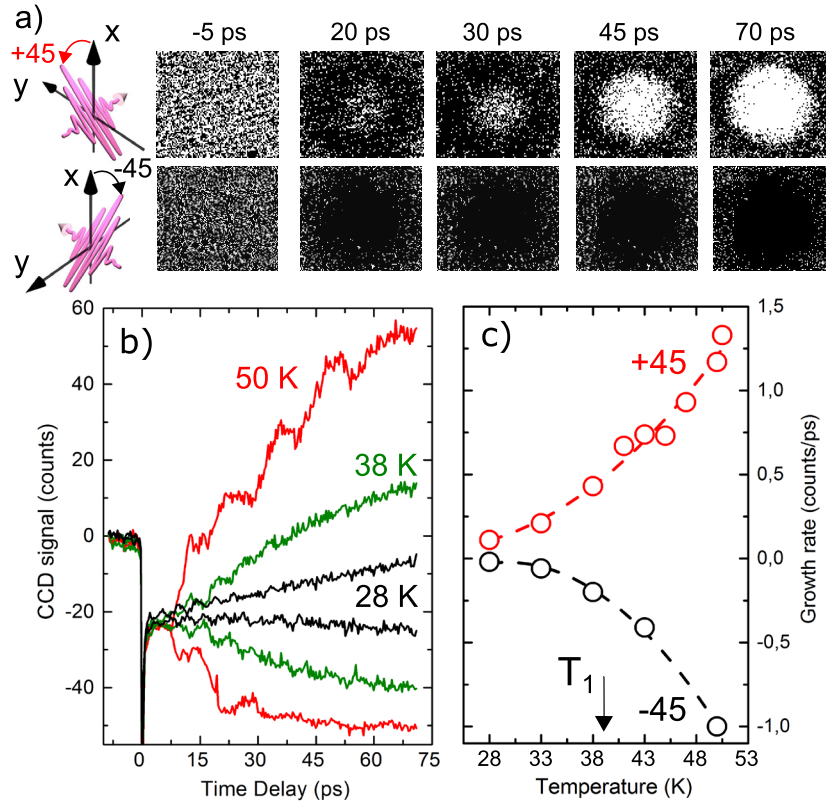
Figure 3. (a) Time-resolved magneto-optical images of the photo-induced dynamics in $HoFeO_3$ for two azimuthal polarizations of the pumping light. The images are obtained by taking the difference between the images at the given positive delay and those at negative delay. The bias sample temperature is set to 35 K. (b) The dynamics of the pump-induced magneto-optical signal averaged over the spot for different bias temperatures. Two curves corresponding to the pumping light having polarization ±45 with respect to the *x*-axis are plotted for each temperature. (c) The growth rate of the magneto-optical signal from the dynamics segment which demonstrates nearly linear growth as a function of the sample temperature. The dashed lines are guides to the eye.

magnetic ground state and shows well pronounced hysteretic behavior. This indicates that a change of the sign of the magnetization in the ground state affects the direction of the photo-induced magnetization. To confirm this hypothesis we pumped various areas of the sample without external magnetic field after heating above T_3 and subsequent cooling to the initial temperature. Figure 2(d) shows that pumping the sample at spatially different areas may lead to opposite results. The periodic areas in which white or black photo-induced domains emerge represent the magnetic domain pattern of the Γ_{12} phase. Similarly to [11] the sign of the photo-induced magnetization depends on the initial orientation of the spins and the laser-induced effect change sign upon changing the magnetic domain. Our findings regarding the sign of the photo-induced magnetization can be summarized in a simple form: $\text{sign}(M_z) = \text{sign}(M_x) \cdot \text{sign}(\sin 2\varphi)$. Recently, a similar behavior was reported for the Morin phase transition in $DyFeO_3$ [10]. In that case the degeneracy between two orientations of the photo-induced magnetization was lifted by light-induced excitation of coherent spin precession. To understand the mechanism of the control of the sign of the photo-induced magnetization in $HoFeO_3$, one has to perform time-resolved experiments.

5. Time-resolved dynamics of the photo-induced magnetization

Figure 3(a) demonstrates the dynamics of the photo-induced magnetization for two distinct orthogonal linear polarizations of the pump pulse. We discriminate three main features in the pump-induced dynamics of the magnetization: (i) pronounced time delay preceding the magnetization growth, (ii) coherent high-frequency oscillation, (iii) gradual growth of the magnetization (see figure 3(b)). The phase of the oscillation is sensitive to the polarization of the pumping light in the same extent as the sign of the magnetization growth. This observation is a strong indication that in $HoFeO_3$, similarly to other orthoferrites [9–11, 20], light-induced coherent spin precession can lift the degeneracy between the magnetic states with magnetizations 'up' or 'down', respectively.

Further we limit our analysis of magnetization dynamics to the cases of the pump polarizations corresponding to the angles $\varphi = \pm 45$ degrees. We extracted the value for the growth rate of the magneto-optical signal from those dynamic segments which demonstrate nearly linear growth. Figure 3(c) shows that for the growth rate, the polarization sensitive contribution to the magnetization dynamics persists even down to 28 K.
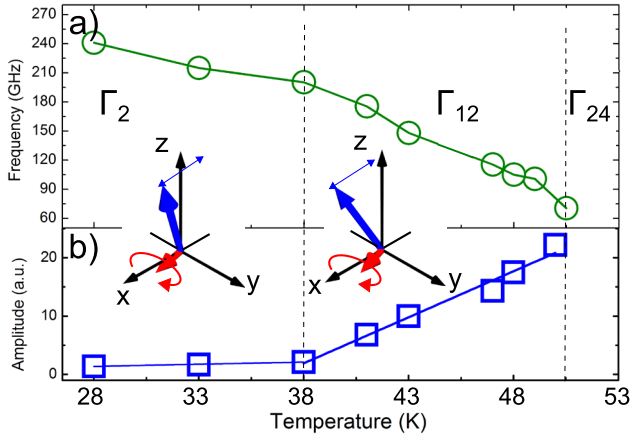
Figure 4. (a) The frequency f_{FM} of the photo-induced oscillations as a function of the sample temperature. (b) Amplitude of the oscillations as a function of the sample temprature. The dashed lines separate regions of stable magnetic configurations of HoFeO$_3$. The insets are schematic representations of the quasiferromagnetic spin mode for various magnetic configurations.

This is far below than the lower border of the Γ_{12} phase. It implies that the laser excitation can drive not only a single transition from $\Gamma_{12} \rightarrow \Gamma_{24}$ but a cascade of phase transitions $\Gamma_2 \rightarrow \Gamma_{12} \rightarrow \Gamma_{24} \rightarrow \Gamma_4$.

In the following sections we discuss all these features in detail.

5.1. High-frequency coherent quasiferromagnetic soft mode

The frequency of the photo-induced oscillation f_{FM} shows a softening down to 60 GHz if the sample temperature approaches T_2, see figure 4(a). This temperature behavior in the vicinity of the phase transition from the Γ_{12} to the Γ_{24} phases is a hallmark of the so-called quasiferromagnetic mode of the spin oscillations in HoFeO$_3$ [15]. The oscillation is a precession of the net magnetization around the equilibrium orientation, so that time-varying components L_x, M_x and M_y emerge.

In order to understand the mechanism of the light-induced excitation of the quasiferromagnetic mode we employed a phenomenological free energy approach [14]. The lowest order term $\Delta\Phi$ which is allowed by the magnetic symmetry of the low-temperature phases (Γ_2 and Γ_{24}) which describes interaction of linearly polarized light, having electric field component in the (0 0 1) crystallographic plane, with spins reads [13]:

$$\Delta\Phi = \frac{1}{16\pi}(\mathscr{A}_{xyxy}L_xL_y + \mathscr{B}_{yzxy}L_yM_z + \mathscr{B}_{zyxy}L_zM_y)(\mathscr{E}_x\mathscr{E}_y^* + c.c.) \quad (2)$$

Here $\mathscr{A}_{xyxy}$, $\mathscr{B}_{yzxy}$ and $\mathscr{B}_{zyxy}$ are phenomenological parameters. The second factor in equation (2) is convenient to rewrite as: $\frac{1}{16\pi}(\mathscr{E}_x\mathscr{E}_y^* + c.c.) = I(t)\sin 2\varphi$, where $I(t) = \frac{1}{8\pi}|\mathscr{E}|^2$. $\mathscr{E}_x(t)$ and $\mathscr{E}_y(t)$ are time-dependent x and y components of the electric field of the pump pulse, respectively. The light intensity I_0, measured experimentally, is given by $I_0 = \int_{-\infty}^{+\infty} I(t)dt$.

The sigma-model equations [14] are determined by variation of the Lagrangian. For one spin, in the units of the Planck constant $\hbar$ the Lagrangian reads:

$$\mathscr{L} = T + G - W(\mathbf{L}, t)$$
$$T = \frac{1}{2\gamma H_{ex}}\left(\frac{d\mathbf{L}}{dt}\right)^2 \quad G = -\frac{1}{H_{ex}}\left(\mathbf{H}_{eff} \cdot \left(\mathbf{L} \times \frac{d\mathbf{L}}{dt}\right)\right). \quad (3)$$

The first two terms in equation (3) determine the inertial T and the gyroscopic G dynamics of an antiferromagnet. γ is the gyromagnetic ratio. The effective magnetic field $\mathbf{H}_{eff}$ in orthoferrites is given by the sum of the static Dzyaloshinskii field $\mathbf{H}_D = H_D[\mathbf{e}_y \times \mathbf{L}]$ and an effective optomagnetic field created by the light pulse. The opomagnetic field is defined as $\mathbf{h}_{opt} = -\frac{\partial\Delta\Phi}{\partial\mathbf{M}}$, so that in the present case the total effective magnetic field reads:

$$\mathbf{H}_{eff} = \mathbf{H}_D - (\mathscr{B}_{yzxy}L_y\mathbf{e}_z + \mathscr{B}_{zyxy}L_z\mathbf{e}_y)I(t)\sin 2\varphi. \quad (4)$$

The term $W(\mathbf{L}, t)$ within the Lagrangian formalism means an effective 'potential energy' written for the antiferromagnetic vector. The presence of this term determines the inertial features of the spin dynamics [11, 21]. It consist of the phenomenological free energy, the general expression for which, for the case of the orthoferrites, can be found in [22], and light-induced dynamical contribution. In our case the light-induced contribution within the sigma-model formalism acquires the form:

$$\Delta W(t) = \left(\mathscr{A}_{xyxy} - \mathscr{B}_{yzxy} \cdot \frac{H_D}{H_{ex}}\right)L_xL_y \cdot I(t)\sin 2\varphi. \quad (5)$$

Further we will consider contributions into magnetization dynamics from the gyroscopic and the inertial terms, independently. Here we start with the inertial part. The dynamical Lagrange–Euler equations of motion, written for each projection of the antiferromagnetic vector L_i read:

$$\frac{1}{\gamma H_{ex}}\frac{d^2L_x}{dt^2} - \frac{\partial W}{\partial L_x} = \left(\mathscr{A}_{xyxy} - \mathscr{B}_{yzxy} \cdot \frac{H_D}{H_{ex}}\right)L_y \cdot I(t)\sin 2\varphi$$

$$\frac{1}{\gamma H_{ex}}\frac{d^2L_y}{dt^2} - \frac{\partial W}{\partial L_y} = \left(\mathscr{A}_{xyxy} - \mathscr{B}_{yzxy} \cdot \frac{H_D}{H_{ex}}\right)L_x \cdot I(t)\sin 2\varphi$$

$$\frac{1}{\gamma H_{ex}}\frac{d^2L_z}{dt^2} - \frac{\partial W}{\partial L_z} = 0. \quad (6)$$

It is clearly seen that the action of light results in a time-dependent 'driving force'. This mechanism effectively acts in phases which are characterized by non-zero x and y components of the vector $\mathbf{L}$. In the phase with $L_x \neq 0$ this results in:

$$\frac{dL_y}{dt}(+0) = \left(\mathscr{A}_{xyxy} - \mathscr{B}_{yzxy} \cdot \frac{H_D}{H_{ex}}\right)L_x \cdot I_0\sin 2\varphi. \quad (7)$$

For the orthogonal phase, characterized by $L_y \neq 0$, this results in:

$$\frac{dL_x}{dt}(+0) = \left(\mathscr{A}_{xyxy} - \mathscr{B}_{yzxy} \cdot \frac{H_D}{H_{ex}}\right)L_y \cdot I_0\sin 2\varphi. \quad (8)$$
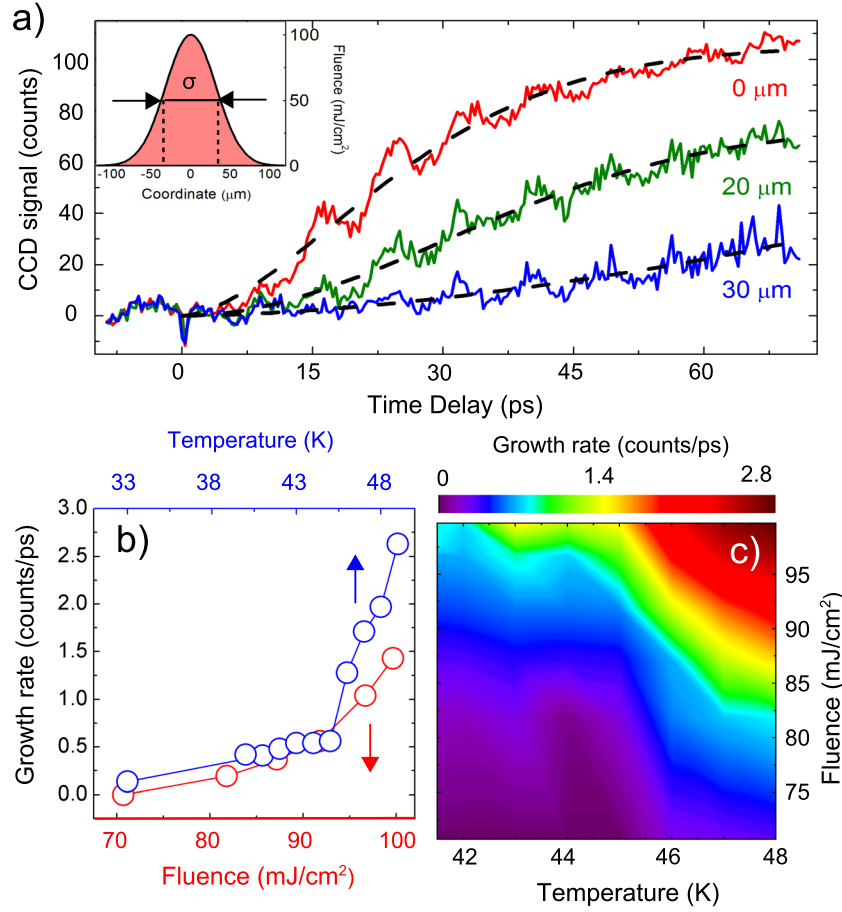
Figure 5. (a) Time-resolved traces of the magneto-optical signal for images of the photo-induced dynamics in HoFeO$_3$. The plots are obtained by taking the difference between those measured for two azimuthal polarizations of the pumping light $\varphi = +45$ and $\varphi = -45$. The sample temperature is 32 K. The inset shows the simulated spatial profile of the pump pulse. The dashed lines are guides to the eye. (b) The phase diagram of the magnetization growth rate as a function of the pump-fluence and the temperature. The color code represents the measured value of the growth rate. (c) Comparison of the the magnetization growth rate dependencies on the fluence and the temperature.

As a result, we show that the magnetization dynamics in HoFeO$_3$ can be launched via the inertial mechanism by means of linearly polarized light in phases which are characterized by non-zero x and y components of **L**. The efficiency of the excitation is controlled by the azimuthal angle φ. The inertial mechanism explains the symmetry of the soft mode excitation in the Γ_{12} phase, for which $L_y \neq 0$. In contrast, this result anticipates that linearly polarized light incident along the z-axis cannot trigger the magnetization dynamics in the Γ_2 phase, which is solely characterized by $L_z \neq 0$. Indeed, for temperatures below 38 K the slope of the amplitude dependence demonstrates a pronounced change (see figure 4(b)). This temperature nearly matches with T_1. Below T_1, despite a significant drop, the amplitude of the oscillations remains non-zero and nearly temperature-independent.

The excitation of the spin dynamics in the Γ_2 phase cannot be explained within the inertial mechanism. In order to describe the light-induced spin dynamics in this phase, we took into account the gyroscopic term in the Lagrangian, see equation (3). This term in the Γ_2 phase reads:

$$\Delta G = -\frac{1}{H_{\text{ex}}} \Big\{ \mathscr{B}_{yzxy} L_y \Big(L_x \frac{\text{d}L_y}{\text{d}t} - L_y \frac{\text{d}L_x}{\text{d}t} \Big)$$
$$+ \mathscr{B}_{zyxy} L_z \Big(L_z \frac{\text{d}L_x}{\text{d}t} - L_x \frac{\text{d}L_z}{\text{d}t} \Big) \Big\} I(t) \sin 2\varphi. \quad (9)$$

Taking into account that $L_z \gg L_x, L_y$, which is valid for magnetization dynamics in the Γ_2 phase, equation (9) can be reduced to:

$$\Delta G \approx -\frac{1}{H_{\text{ex}}} \mathscr{B}_{yzxy} L_z^2 \frac{\text{d}L_x}{\text{d}t} I(t) \sin 2\varphi. \quad (10)$$

The Lagrange–Euler equation accounting for the gyroscopic term in the Γ_2 phase can be written as a closed equation for L_x only and reads:

$$\frac{1}{\gamma H_{\text{ex}}} \frac{\text{d}^2 L_x}{\text{d}t^2} - \frac{\partial W}{\partial L_x} = -\frac{1}{\gamma H_{\text{ex}}} \mathscr{B}_{zyxy} \frac{\text{d}I(t)}{\text{d}t} \sin 2\varphi. \quad (11)$$

The time-dependent optomagnetic effective field via the gyroscopic term leads to the initial deflection of the magnetization [23, 24]:
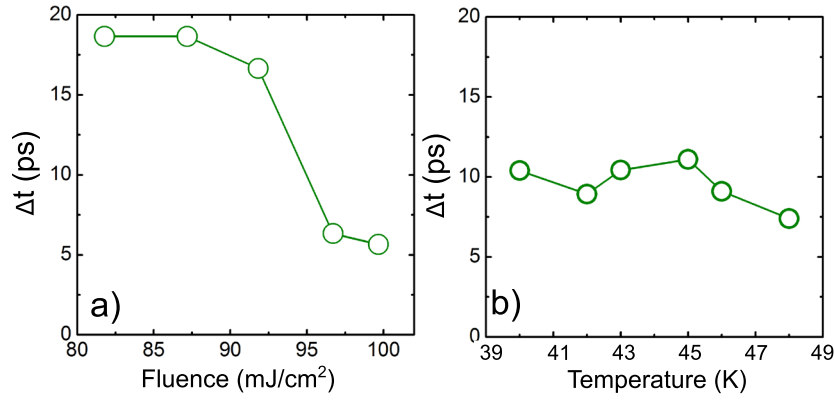
Figure 6. (a) The pump polarization-independent delay Δt in the photo-induced dynamics of the magnetization for various fluences of the pump. (b) The same value for various bias temperatures of the sample.

$$L_x(+0) = -\mathscr{B}_{zyxy}I_0 \sin 2\varphi. \tag{12}$$

Thus we have shown that the quasiferromagnetic mode can be excited by means of light in both Γ_2 and Γ_{12} phases. It is clearly seen that different mechanisms result in different efficiencies of the excitation of the spin oscillations.

5.2. Thermally driven dynamics of the photo-induced magnetization

The magnetization dynamics, averaged over the photo-induced domain, for different temperatures is shown on figure 3(b). The growth rate increases approaching T_2 and shows a pronounced non-linear temperature behavior (figure 3(c)). Interestingly, no peculiarities in the growth rate are observed once the temperature passes T_1. This indicates that the factor which promotes the growth is most likely not sensitive to the magnetic order itself.

To clarify the origin of the magnetization growth, we compared the rate of the growth measured for various temperatures with the same value obtained for various fluences of the pump. The fluence dependence can be easily extracted from the digital images, if one accounts for the Gaussian distribution of the fluence in the spatial profile of the pumping light (see inset in figure 5(a)). One can see that the fluence dependence, shown on figure 5(a), demonstrates striking similarities with the temperature dependence (see figure 3(b)). A comparison of the fluence and temperature dependencies of the growth rate, shown on figure 5(b), demonstrates that they have the same trend. We plotted a color map (figure 5(c)) of the magnetization growth rate, measured in CCD counts per second. The color map shows that in the vicinity of the transition from the Γ_{12} to the Γ_{24} phase the fluence and the temperature are nearly proportional with the proportionality 4 mJ cm^{-2} K. This experiment demonstrates that the photo-induced growth of the magnetization in HoFeO$_3$ is solely driven by the pump-induced increase in the lattice temperature. Indeed, taking the specific heat $C = 10$J (K·mol)$^{-1}$ [16], mass density $\rho \approx 10$ g cm^{-3} [25], atomic mass $A = 269$, the irradiation of the sample with the pump pulse having energy $E = 4\mu$J results in a heating ΔT:

$$\Delta T = \frac{E \cdot A}{C \cdot \rho \cdot \pi(0.5\sigma)^2 \cdot d} \cdot \mathrm{e}^{-\alpha d} \approx 17 \text{ K}. \tag{13}$$

Note, that the estimate of the laser-induced heating given in [11], exceeds the one obtained here. This can be related to an error in the definition of spot size in the earlier works. Performing imaging, the errors are less probable. However, in both cases it was concluded that the temperature raise defines incoherent dynamics of the magnetization. This incoherent magnetization dynamics can be attributed to the temperature-driven growth of the nuclei of the high-temperature phases (Γ_{24} or Γ_4) in the volume of the initial phase. The initial temperature defines the initial number of nuclei and their growth rate. This may explain the experimentally observed non-linear dependency of the magnetization growth rate as a function of temperature (see figures 3(c) and 5(b)).

Interestingly, the observed temperature dependence of the magnetization dynamics along with the fluence dependence are qualitatively similar to the recently observed ultrafast light-induced first-order metal–insulator transition in V$_2$O$_3$ [26]. Despite the differences in the microscopic nature of these transitions, the light-induced dynamics of the order parameter are qualitatively the same. This points to the universality of the ultrafast dynamics of the order parameter triggered at first-order phase transitions.

5.3. Polarization-independent delay in the growth of the photo-induced magnetization

The time delay Δt which precedes the onset of the photo-induced magnetization is a conspicuous feature visible in the pump–probe time traces (see both figures 3(a) and 5(a)). It reaches values up to 20 ps for low fluences of the pumping light. Interestingly, while Δt is a strong function of the pump fluence, it is nearly independent of the sample temperature (figure 6). Most likely this is an experimental artifact caused by a transient crystallographic birefringence induced by the pump in the medium. The birefringence can negatively affect the sensitivity of the polarimeter used in this work, making the actual dynamics invisible. In particular, here we cannot see an onset of the inertial motion of the spins as reported in

[11]. Only upon relaxation of the birefringence on the scale of 10 ps, the laser-induced spin dynamics can be distinguished in the measurements.

6. Conclusions

We have shown that an ultrashort laser pulse can trigger spin reorientation in HoFeO$_3$ over 90 degrees. The direction of the magnetization in the transient photo-induced state can be switched from 'up' to 'down' by varying the linear polarization of the pump pulse with respect to the crystallographic axes. The same effect can be achieved if one changes the sign of the magnetization in the initial phase. We show that the ultrafast time-resolved dynamics of the photo-induced magnetization reveals pronounced stages of nucleation and subsequent growth of the new phase. Comparing the dynamics of the magnetization for various temperatures and fluences of the pumping light, it is shown that the magnetization growth is an incoherent process driven by the laser heating. The sign of the magnetization in the growing domains is defined by the polarization of the pump and the magnetization of the initial state. Again we confirm that the mechanism of the control of the route of the phase transition is based on excitation of coherent spin precession, which predefines the sign of the magnetization in the nuclei. The striking difference in the amplitude of the coherent spin precession in the magnetic phases Γ_2 and Γ_{24} is related to the efficiency of the excitation mechanisms acting independently in these phases: inertial and the gyroscopic, respectively.

References

[1] Beaurepaire E, Merle J C, Daunois A and Bigot J Y 1996 *Phys. Rev. Lett.* **76** 4250
[2] Kimel A V, Kirilyuk A, Usachev P A, Pisarev R V, Balbashov A M and Rasing T 2005 *Nature* **435** 655
[3] Nova T F, Cartella A, Cantaluppi A, Först M, Bossini D, Mikhaylovskiy R, Kimel A, Merlin R and Cavalleri A 2017 *Nat. Phys.* **13** 132–6
[4] Baierl S, Hohenleutner M, Kampfrath T, Zvezdin A, Kimel A, Huber R and Mikhaylovskiy R 2016 *Nat. Photon.* **10** 715
[5] Ostler T *et al* 2012 *Nat. Commun.* **3** 666
[6] Von Korff Schmising C *et al* 2014 *Phys. Rev. Lett.* **112** 217203
[7] Graves C *et al* 2013 *Nat. Mat.* **12** 293
[8] Stupakiewicz A, Szerenos K, Afanasiev D, Kirilyuk A and Kimel A 2017 *Nature* **542** 71–4
[9] de Jong J A, Razdolski I, Kalashnikova A M, Pisarev R V, Balbashov A M, Kirilyuk A, Rasing T and Kimel A V 2012 *Phys. Rev. Lett.* **108** 157601
[10] Afanasiev D, Ivanov B A, Kirilyuk A, Rasing T, Pisarev R and Kimel A 2016 *Phys. Rev. Lett.* **116** 097401
[11] Kimel A V, Ivanov B A, Pisarev R V, Usachev P A, Kirilyuk A and Rasing T 2009 *Nat. Phys.* **5** 727
[12] Srinivasan G and Slavin A N 1995 *High Frequency Processes in Magnetic Materials* (Singapore: World Scientific)
[13] Turov E A, Kolchanov A V, Kurkin M I, Mirsaev I F and Nikolaev V V 2010 *Symmetry and Physical Properties of Antiferromagnets* (Cambridge: Cambridge International Science)
[14] Ivanov B A 2014 *Low Temp. Phys.* **40** 91
[15] Balbashov A, Volkov A, Lebedev S, Mukhin A and Prokhorov A 1985 *Zh. Eksp. Teor. Fiz.* **88** 974
[16] Bhattacharjee A, Saito K and Sorai M 2002 *J. Phys. Chem. Solids* **63** 569
[17] Zeng X, Fu X, Wang D, Xi X, Zhou J and Li B 2015 *Opt. Express* **23** 31956
[18] Chatterji T, Meven M and Brown P 2016 arXiv:1604.08349
[19] Kimel A V, Pisarev R V, Hohlfeld J and Rasing T 2002 *Phys. Rev. Lett.* **89** 287401
[20] Kurihara T, Watanabe H, Nakajima M and Suemoto T 2016 *41st Int. Conf. on Infrared, Millimeter, and Terahertz waves* (IEEE) pp 1–2
[21] Iida R, Satoh T, Shimura T, Kuroda K, Ivanov B A, Tokunaga Y and Tokura Y 2011 *Phys. Rev.* B **84** 064402
[22] Barýakhtar V G, Ivanov B A and Chetkin M V 1985 *Sov. Phys.—Usp.* **28** 563
[23] Galkin A Y and Ivanov B A 2008 *JETP Lett.* **88** 249
[24] Satoh T, Cho S J, Iida R, Shimura T, Kuroda K, Ueda H, Ueda Y, Ivanov B A, Nori F and Fiebig M 2010 *Phys. Rev. Lett.* **105** 077402
[25] Belokolos E and Safronkov O Y 1992 *J. Phys.: Condens. Matter* **4** 8617
[26] Abreu E, Wang S, Ramírez J G, Liu M, Zhang J, Geng K, Schuller I K and Averitt R D 2015 *Phys. Rev.* B **92** 085130